Jpn. J. Appl. Phys. Vol. 42 (2003) pp. 3239–3245
Part 1, No. 5B, May 2003

Measurement of Rapid Variation in Ultrasound Backscattering During Change in Thickness of Tissue Phantom

Hiroshi KANAI*,†, Yoshiro KOIWA‡, Shin'ichi KATSUMATA†, Naoyuki IZUMI† and Motonao TANAKA§

Department of Electronic Engineering, Graduate School of Engineering, Tohoku University, Aramaki-aza-Aoba 05, Sendai 980-8579, Japan

(Received November 18, 2002; accepted for publication March 12, 2003)

The cyclic variation in ultrasound integrated backscatter (IB) during one cardiac cycle offers potential for evaluation of myocardial contractility. Since there is large motion due to the heartbeat in the heart wall, in the conventional method, the position of the region of interest (ROI) for calculating the IB is manually set for each timing during one heartbeat. Moreover, change in the size of the ROI during contraction and relaxation of the myocardium is not considered. In this paper, a new method is proposed for automatic tracking of the position and the size of the ROI. Rapid components, which are detected by increasing the spatial and time resolutions to 1 mm and 200 μs, respectively, highly depend on the instantaneous velocity of the ROI. These components are the result of interference between the waves reflected by the ROI and those reflected by scatterers other than the ROI. By separately estimating the bias component, these interfering components which cause interference are eliminated. By applying the proposed method to a sponge phantom, which was cyclically depressed in a water tank, and to the posterior wall of the heart of a healthy subject, the interference components were sufficiently suppressed and the IB signals were obtained with high spatial and time resolution. [DOI: 10.1143/JJAP.42.3239]

KEYWORDS: phased tracking method, integrated backscatter, sponge phantom, contraction and relaxation, myocardium contractility, cyclic variation

1. Introduction

One of the ultimate goals of medical ultrasonic research is tissue characterization, that is, to provide supplemental information describing the physical state of the tissue based on a quantitative analysis of interactions between tissue and ultrasound. In previous studies, it was found that ultrasound integrated backscatter (IB) from the myocardium exhibits cyclic variation during one cardiac cycle[1–3] and that the magnitude of such variation was reduced by ischemia.[4] These results suggest that the cyclic variation in ultrasound IB during one cardiac cycle offers potential for evaluation of myocardial contractility. Thus, analysis of the cyclic variation of ultrasound IB has been established as a noninvasive and sensitive method for evaluating intrinsic left ventricular (LV) contractile performance and for detecting myocardial viability.[5–8]

Since there is large motion due to the heartbeat in the heart wall, in conventional measurement, the position of the region of interest (ROI) for detecting IB is manually set at each timing during one heartbeat. Furthermore, the thickness of the heart wall changes during contraction and relaxation of the myocardium. However, the change in size of the ROI is completely ignored in conventional measurement.

In this paper, by introducing the phased tracking method,[9,10] each displacement of multiple points, which are set at intervals of 0.375 mm in the heart wall along an ultrasonic beam, is accurately tracked. By setting the ROI between two adjacent points, the instantaneous position and the size of the ROI are automatically traced.

Since spatial resolution and time resolution were increased to 1 mm and 200 μs, respectively, in this study, components which rapidly varied were observed in the IB signal for the first time. Such rapidly varying components highly depend on the speed of displacement of the ROI and these components are the result of interference between the waves reflected by the ROI and those reflected by the other scatterers. Proposed herein is a method for eliminating these rapid components in which by the bias component in the quadrature demodulated signal of the received radio frequency (RF) signal, is estimated.

By applying the proposed method to a sponge phantom, which was cyclically depressed in a water tank, the interference components were sufficiently suppressed. Next, the method was applied to the LV posterior wall of a healthy subject in *in vivo* experiments. The IB signal was measured with high time resolution and high spatial resolution, an impossibility with the conventional method.

2. Method for Maintaining the Same ROI in Detection of the IB

2.1 Principle for tracking displacement in the heart wall

RF pulses with an angular-frequency of $\omega_0 = 2\pi f_0$ are transmitted at a time interval of ΔT from an ultrasonic transducer. The ultrasonic pulse, reflected by an object with a depth of x, is received by the same transducer. The phase difference $\Delta\theta(t;x)$ between the received signal $y(t;x)$ and the subsequently received signal $y(x;t+\Delta T)$ is given by

$$\begin{aligned}\Delta\theta(t;x) &= \theta(x;t+\Delta T) - \theta(t;x) \\ &= \frac{2\omega_0}{c_0}\Delta x(t),\end{aligned} \tag{2.1}$$

where $\theta(t;x)$ is the phase of the received signal $y(t;x)$, $\Delta x(t) = x(t+\Delta T) - x(t)$ is the displacement of the object during the period ΔT from a time t, and c_0 is the acoustic velocity in the human body. By dividing the movement Δx by the period ΔT, the average velocity $v(t+\frac{\Delta T}{2})$ of the object during the period ΔT is given by

*E-mail address: hkanai@ecei.tohoku.ac.jp
†Present address: Department of Electronic Engineering, Graduate School of Engineering, Tohoku University Aramaki-aza-Aoba 05, Sendai 980-8579, Japan.
‡Present address: First Department of Internal Medicine, Graduate School of Medicine, Tohoku University Seiryou-machi, Aoba-ku, Sendai 980-8574, Japan.
§Present address: Tohoku Welfare Pension Hospital, Fukumuro 1-12-1, Miyagino-ku, Sendai 983-8512, Japan.

$$\widehat{v}\left(t+\frac{\Delta T}{2}\right)=\frac{\Delta x(t)}{\Delta T}=\frac{c_0}{2\omega_0}\frac{\widehat{\Delta\theta}(t;x)}{\Delta T}, \tag{2.2}$$

where the phase difference $\widehat{\Delta\theta}(t;x)$ is accurately determined by the constraint least-squares approach based on the complex cross-correlation between the quadrature demodulated signals $y(t;x)$ and $y(x;t+\Delta T)$ for suppressing noise components under the constraint that the signal waveform is invariant during ΔT and that only the signal phase can change.[9] By multiplying the resultant velocity $\widehat{v}(t+\frac{\Delta T}{2})$ by the period ΔT, the next depth $\widehat{x}(t+\Delta T)$ is estimated by

$$\widehat{x}(t+\Delta T)=\widehat{x}(t)+\widehat{v}\left(t+\frac{\Delta T}{2}\right)\times\Delta T. \tag{2.3}$$

By moving the depth of the object along the direction of the ultrasonic beam based on the resultant object depth $\widehat{x}(t+\Delta T)$ by $\widehat{v}(t+\frac{\Delta T}{2})\times\Delta T$, the displacement of the object is tracked, and then the velocity signal $\widehat{v}(t+\frac{\Delta T}{2})$ on the tracked large motion can be accurately estimated.[9] This procedure is called the *phased tracking method*.

The LV wall shows large motion with an amplitude of about 10 mm during the cardiac cycle, and the LV wall shows periodic thickening and thinning along with myocardial contraction and relaxation, the magnitude of which is about 30% of the thickness in healthy subjects.[10]

2.2 IB detection of the same ROI

The difference between position $\widehat{x}_i(t)$ of the ith point and position $\widehat{x}_{i+1}(t)$ of the $(i+1)$th point set along an ultrasonic beam shows the *local thickness* at every instant of time during one cardiac cycle, where $\widehat{x}_{i+1}(t)>\widehat{x}_i(t)$. Let us define i-th ROI as the region between these two positions $\widehat{x}_i(t)$ and $\widehat{x}_{i+1}(t)$ as shown in Fig. 1. Thus, the IB value, $IB_i(t)$, of the i-th ROI is given by

$$IB_i(t)=10\log_{10}\frac{1}{\widehat{x}_{i+1}(t)-\widehat{x}_i(t)}\int_{\widehat{x}_i(t)}^{\widehat{x}_{i+1}(t)}|z(t;x)|^2\mathrm{d}x, \quad [\mathrm{dB}] \tag{2.4}$$

where $z(t;x)$ is the quadrature demodulated signal of the ultrasonic pulse $y(t;x)$ reflected by the object at position x at time t. Thus, the spatially averaged squared magnitude of the quadrature demodulated signal is normalized by the instantaneous thickness $\widehat{x}_{i+1}(t)-\widehat{x}_i(t)$ of the i-th ROI as shown in Fig. 1.

2.3 Cause of the rapid change components in IB signals

In actual measurement, the received signal $y(t;x)$ has some components $y_1(t;x)$ other than the ultrasonic pulse $y_0(t;x)$ reflected by the ROI. These components, $y_1(t;x)$, are the result of the ultrasonic pulse reflected at *the other points* due to the side lobe or the grating lobe of the ultrasonic transducer as illustrated in Fig. 2. These components, $y_1(t;x)$, interfere with the ultrasonic pulse $y_0(t;x)$ reflected at the ROI. The ROI is set in the heart wall and has large motion due to the heartbeat. On the other hand, it can be assumed that the position of *the other points* do not change so much. In this case, the IB has rapid change components as explained below.

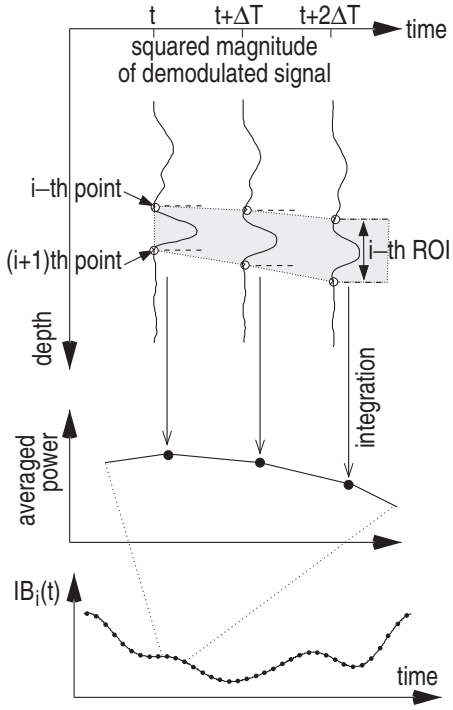

Fig. 1. Illustration of the proposed method for calculating the IB by tracking the instantaneous position and thickness of the ROI.

First, an optimal case is considered, that is, the received signal $y(t;x)$ contains only the ultrasonic pulse $y_0(t;x)$ reflected by the scatterers in the ROI at position x. To describe the displacement of the ROI, the quadrature demodulated signal $z(t;x)$ of $y(t;x)$ is described by $z(t;x)=z_0\exp\{j\theta(t)\}$, where $\theta(t;x)$ denotes the phase delay due to the two-way transmission of the ultrasonic pulse from

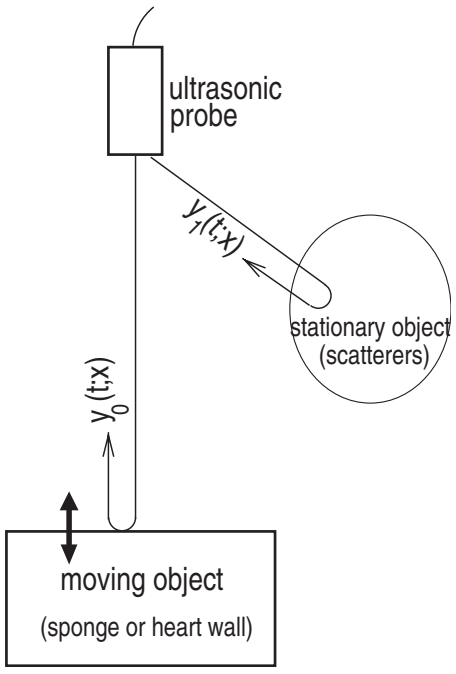

Fig. 2. Interference between the ultrasonic pulse reflected by a moving object and that reflected by scatterers in a stationary object due to the side lobe or the grating lobe of the ultrasonic probe.

the ultrasonic probe to the object at position $x(t)$ and time t, and z_0 is the amplitude of the received pulse. When the ROI follows the position of the same object in the heart wall as illustrated in Fig. 2 and the change in attenuation can be negligible for a short period, z_0 can be assumed to be constant. Thus, the magnitude of the quadrature demodulated signal, $|z(t;x)|$, in eq. (2.4) keeps the same value, namely,

$$|z(t;x)| = z_0, \tag{2.5}$$

which shows that the quadrature demodulated signal $z(t;x)$ rotates around the circumference of the circle the circle with a radius of z_0 as illustrated in Fig. 3(a). The center of the circle coincides with the origin.

Secondly, when the received signal $y(t;x)$ contains the ultrasonic pulse $y_1(t;x)$ reflected by *the other points* as in Fig. 2, let us roughly describe the component as z_1 and assume that it does not change for a short period of time. Thus, the quadrature demodulated component $z(t;x)$ of the received signal $y(t;x)$ is described by $z(t;x) = z_0 \exp\{j\theta(t)\} + z_1$. Dividing z_1 into the real part z_{R1} and the imaginary part z_{I1}, the magnitude $|z(t;x)|$ is given by

$$\begin{aligned}|z(t;x)| &= |z_0 \exp\{j\theta(t;x)\} + z_1| \\ &= \sqrt{(z_0 \cos\theta(t;x) + z_{R1})^2 + (z_0 \sin\theta(t;x) + z_{I1})^2}.\end{aligned} \tag{2.6}$$

The center of the circle shifts from the origin by the "bias" component $z_1 = (z_{R1}, z_{I1})$ as illustrated in Fig. 3(b). Thus, the magnitude $|z(t;x)|$ of the received signal, which coincides with the distance of the point from the origin, changes according to the rotation of the point around the circumference of the circle. The displacement of the ROI by the wave length λ of the ultrasound with a frequency of f_0 Hz corresponds to the rotation of the point by 2π radian in the circle. In the heart wall, during one cardiac cycle, the displacement is roughly 10 mm, which corresponds to $10\,\text{mm} \times 2\pi \times 2f_0/c_0 \approx 49 \times 2\pi$ radian, where $f_0 = 3.75$ MHz. Therefore, the components with rapid change occur at the magnitude of $z(t;x)$ of eq. (2.4). This phenomenon occurs not only for quadrature demodulated signal $z(t;x)$ but also for the original RF signal $y(t;x)$.

2.4 Correction of rapid change components in IB signals

By assuming that the position of the other point does not change, we can estimate component z_1 as follows. We set the region R_{z1} in the lumen close to the surface of the wall of the object along an ultrasonic beam. The component z_1 is estimated from the quadrature demodulated signal $z(t;x)$ averaged over the set region R_{z1}. In the lumen, the received signal $y(t;x)$, reflected by the red blood cell scatterers has almost the same phase value in the quadrature demodulated signal $z(t;x)$ over R_{z1}. Then, the IB value $IB_i(t)$ of the i-th ROI in eq. (2.4) is correctly obtained after the estimated biased component $\widehat{z}_1$ is subtracted from the quadrature demodulated signal $z(t;x)$ at the ROI as follows:

$$IB_i(t) = 10\log_{10}\frac{1}{\widehat{x}_{i+1}(t) - \widehat{x}_i(t)}\int_{\widehat{x}_i(t)}^{\widehat{x}_{i+1}(t)} |z(t;x) - \widehat{z}_1|^2 \mathrm{d}x \quad [\text{dB}] \tag{2.7}$$

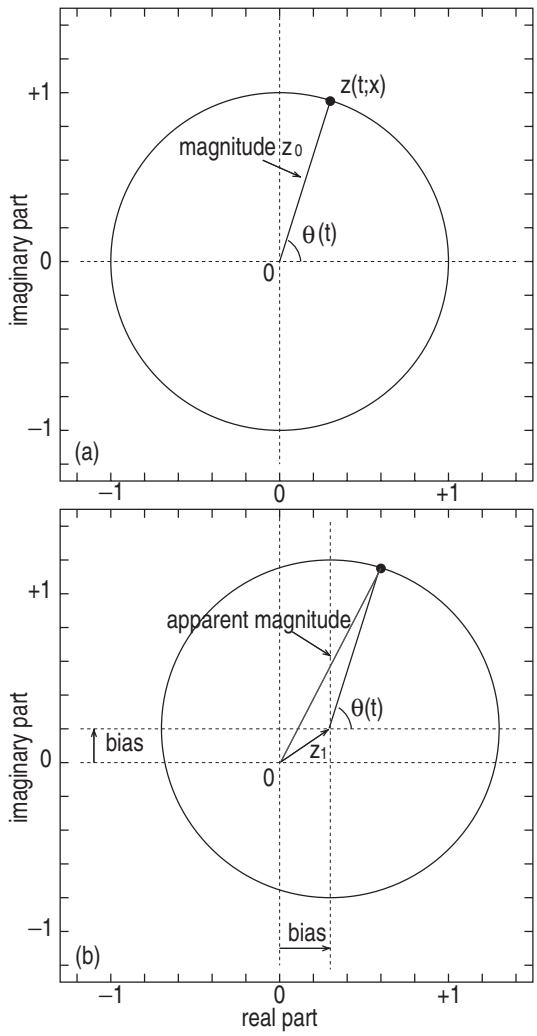

Fig. 3. Magnitude and phase of the quadrature demodulated signal for the case without bias component (a) and with bias component (b).

3. Basic Experiments with Sponge Phantoms

3.1 Experimental setup and tracking results

The above method was applied to a sponge phantom made of polyurethane in a water tank as shown in Fig. 4.

The macroscopic and the microscopic images of the sponge phantom are shown in Fig. 5. The sponge was set under an ultrasonic probe and was manually depressed by about 5 mm at 1-second intervals. A sector-type ultrasonic probe with a frequency of 3.75 MHz was employed. Using conventional ultrasound diagnostic equipment (Toshiba SSH-140A), an ultrasonic pulse was transmitted. The pulse repetition frequency was 4.5 kHz. The pulse reflected by the scatterers in the sponge was received by the same probe. After being amplified and quadrature demodulated, the resultant signal $z(t;x)$ was A/D converted at a sampling frequency of 10 MHz.

Using a hydrophone, the duration time δt of the radiated ultrasonic pulse at the focal area was determined to be about 1,330 ns, which corresponds to a distance of about $1,500 \times \delta t/2 = 1$ mm in depth direction. Thus, the length of the ROI along the ultrasonic beam was set at 1.05 mm in the following experiments.

Figure 6 shows the results for the sponge. The 14 red lines

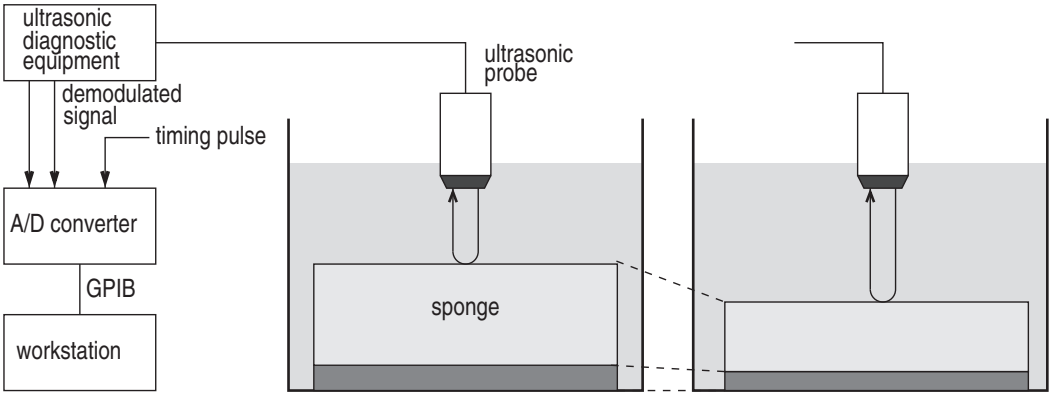

Fig. 4. Experimental setup for repeatedly depressing a sponge phantom in a water tank.

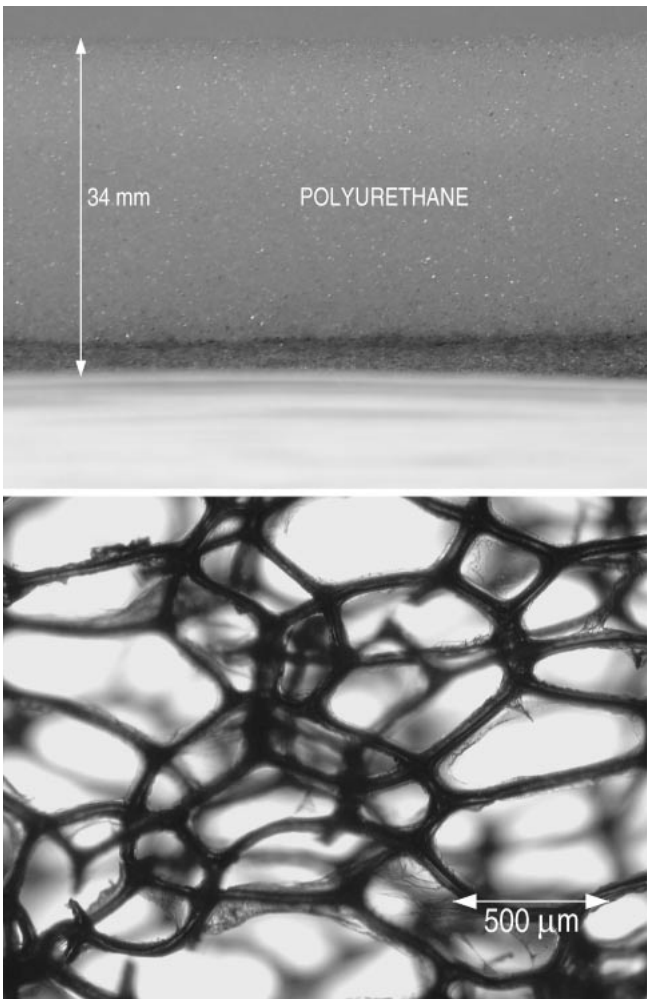

Fig. 5. top: Sponge phantom. bottom: The microscopic view.

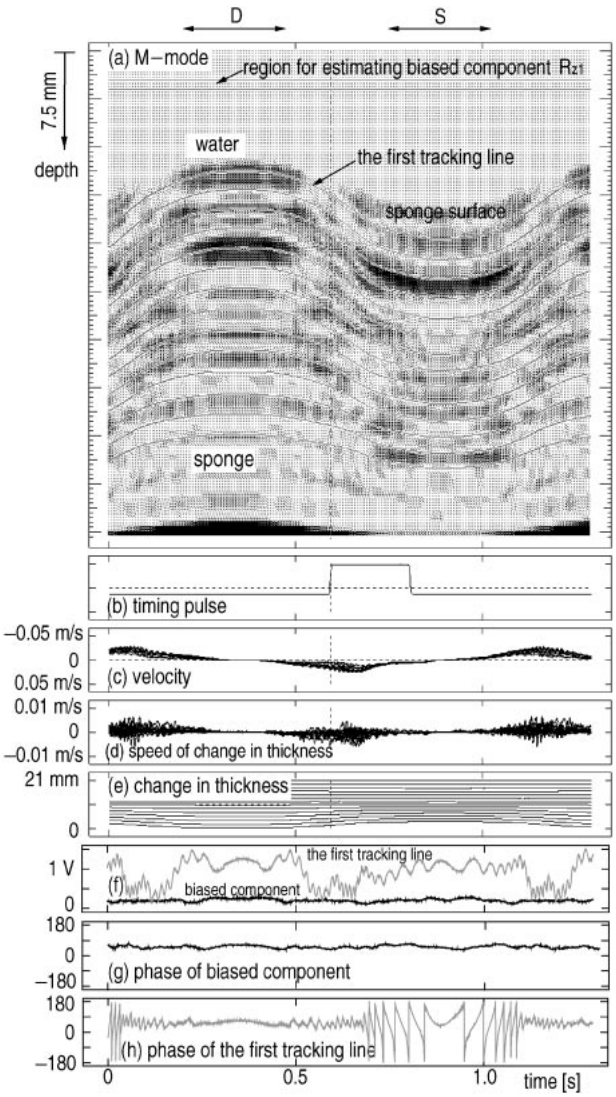

Fig. 6. Tracking results for the sponge. (a) The 14 tracking lines overlaid on the M-mode image. (b) Timing pulses resulting from depression of the sponge. (c) The 14 velocity signals on the 14 tracking lines in (a). (d) Speed of the change in thickness of 13 layers, each of which was the region between two adjacent tracking lines. (e) The change in thickness of the 13 layers. (f) The amplitude of the received signal along the first tracking line near the surface of the sponge and the averaged amplitude of the biased component z_1 obtained in the assigned region R_{z1}. (g) The phase component of the received signal along the first tracking line near the surface of the sponge. (h) The phase component of the biased component z_1.

in the sponge area of Fig. 6(a) show the tracking results overlaid on the M-mode, which was reconstructed from the magnitude of the received quadrature demodulated signals. The amplitude of the change in thickness during one cycle was about 5 mm. Figure 6(b) shows the timing pulses of the contraction of the sponge. Figure 6(c) shows the 14 velocity signals at the 14 points which were followed by the tracking lines in Fig. 6(a). The maximum velocity value is similar to that in the actual human heart.[9] Figure 6(d) shows the speed

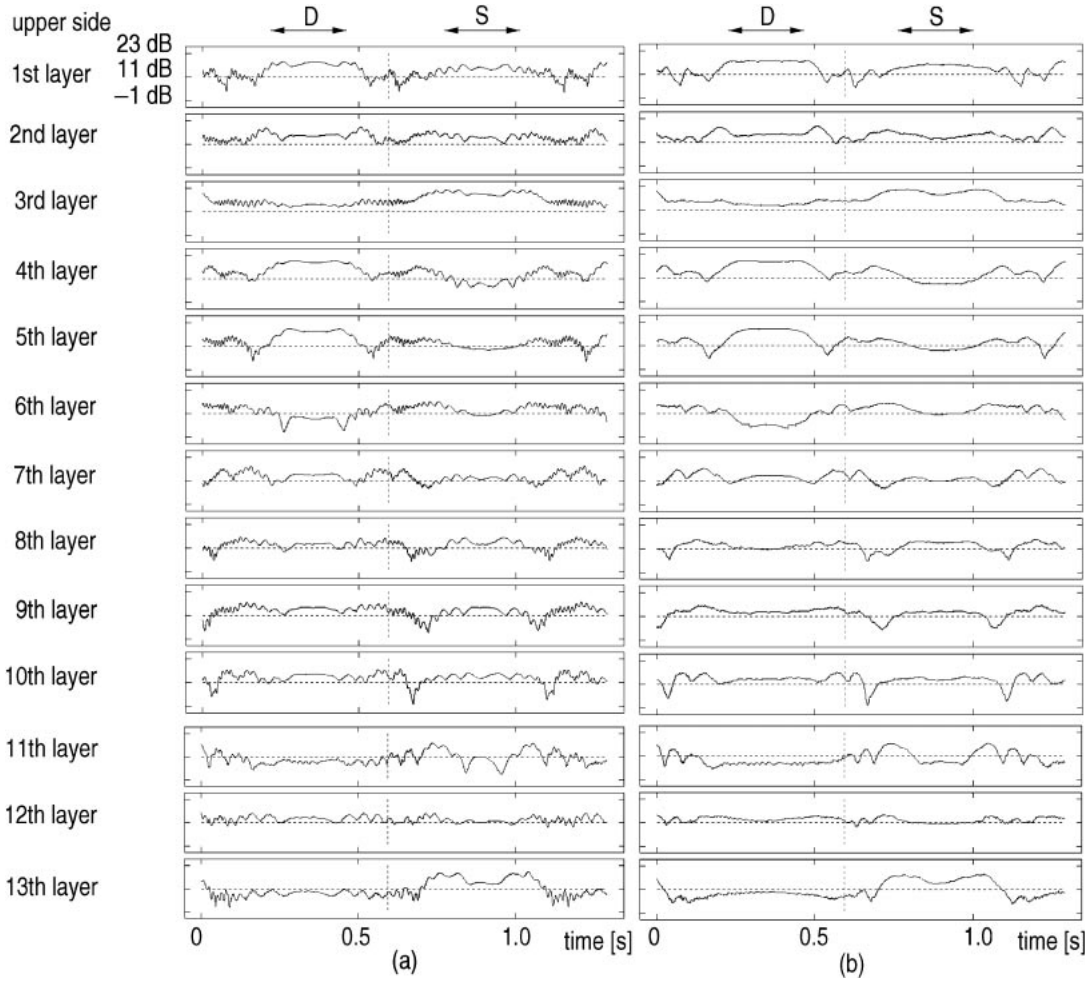

Fig. 7. IB signals for each of the 13 layers for the Sponge. (a) before correction, (b) after correction.

of the change in thickness of the 13 layers (ROI), each of which was defined as the region between the two adjacent tracking lines in Fig. 6(a). Figure 6(e) shows the change in thickness of the 13 layers.

Figure 6(f) shows the amplitude of the received signal along the first tracking line near the surface of the sponge and the averaged amplitude of the biased component z_1 obtained in the assigned region R_{z1} in top of Fig. 6(a). Though the former component changed rapidly during one cycle, the latter bias component z_1 was almost constant. Figures 6(g) and 6(h) show the phase component of the received signal along the first tracking line near the surface of the sponge and that of the biased component z_1. Also for these components, the former component changed rapidly during one cycle but the latter bias component was almost constant. Thus, the correlation between the estimated biased component z_1 and the movement of the sponge was negligible.

3.2 IB signals and their correction

The left-hand side of Fig. 7 shows the IB signal obtained by eq. (2.4) for each of the 13 layers in Fig. 6(a). There were rapid change components from 10 Hz to 80 Hz observed at the times of measurement when the velocity has a large value in Fig. 6(c). The period (D) from 0.2 second to 0.5 second corresponds to the diastole in the heart wall and the period (S) from 0.7 second to 1.0 second corresponds to the systole. By comparing the IB values between the period (S) and the period (D), the envelope of the IB values decreased for both period (S) at from the first layer to the second layer and from the 4th layer to 5th layer. This phenomenon corresponds to the well-known cyclic variation during one cardiac cycle.[11–13] That is, during diastole the fiber in the sponge or intercelluar cement in the myocardium was depressed and the orientation of the fibers became almost parallel. Then, the incident angle of the ultrasound becomes perpendicular to almost all the fibers. Thus, the magnitude of the backscatter increased during diastole. For the other layers, however, these cyclic variation was not observed.

By applying the proposed correction in eq. (2.7) to the same quadrature demodulated signal using the biased component z_1 of Fig. 6(f), the corrected results of the IB signals are shown in the right-hand side of Fig. 7. Almost all the rapid change components in the left-hand side of Fig. 7 were successfully eliminated by the proposed method. Thus, the assumed reason for the occurrence of the interference in the IB is found to be valid.

The fine M-mode images $|z(t;x)|$ before and after the correction are shown in Figs. 8(a) and 8(b), respectively. In Fig. 8(a), rapid change components are seen at the measurement times when the object has large velocity. By the correction, however, these components were eliminated in almost all the layers as shown in Fig. 8(b).

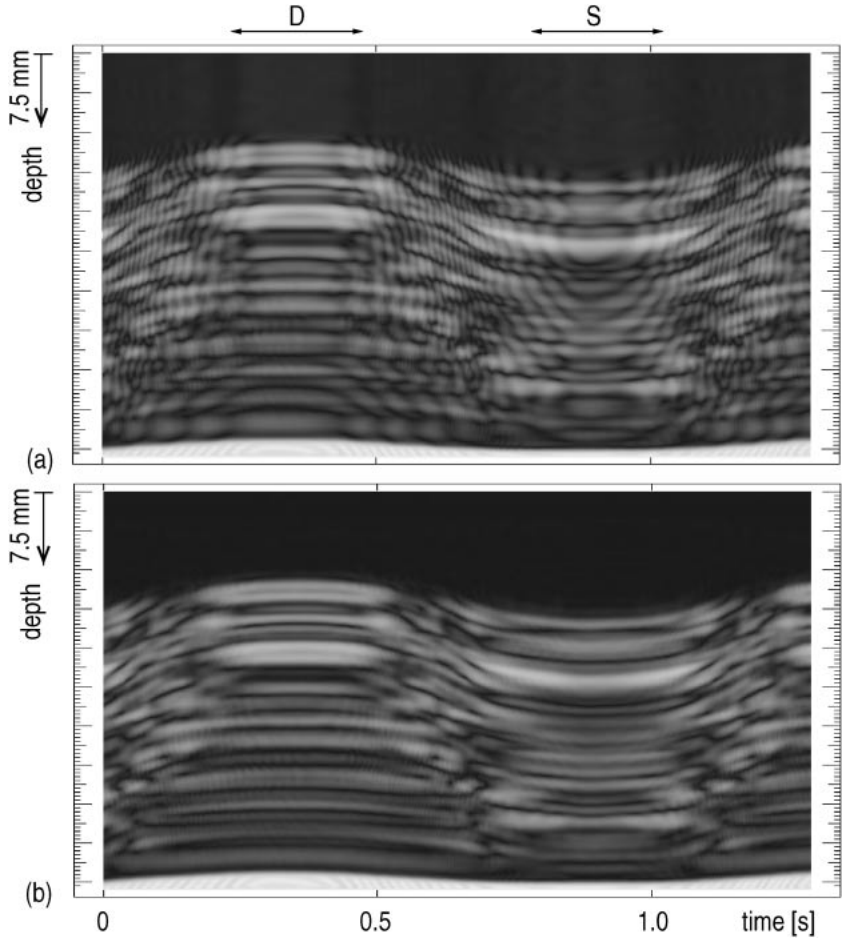

Fig. 8. Fine M-mode images for Sponge (A). (a) before correction, (b) after correction.

4. *In vivo* Experiment for Heart Wall

The same method was applied to the LV posterior wall of the heart of a healthy male subject. The B-mode cross-sectional image is shown in Fig. 9. The employed frequency of the ultrasound was 3.75 MHz. The pulse repetition frequency was 4.5 kHz. The IB signals on the fine M-mode images before and after correction are respectively shown in Figs. 10(a) and 10(b). Figures 11(a) and 11(b) show the IB signal in each layer of the wall before and after correction, respectively.

In Figs. 10(a) and 11(a), rapid change components are apparent, especially at the beginning of the ejection period,

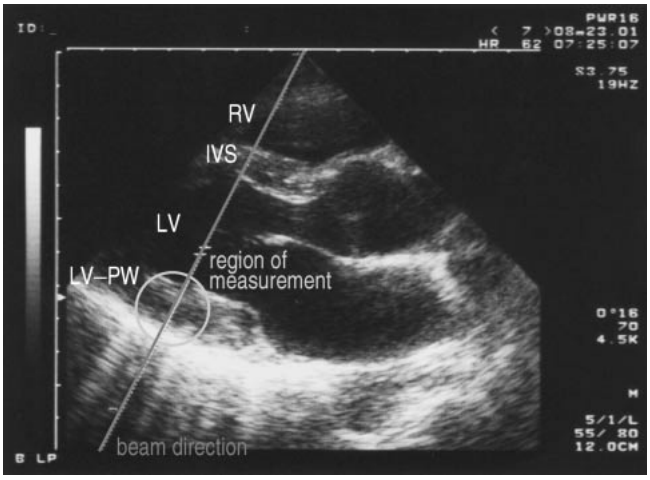

Fig. 9. Cross-sectional B-mode image of the heart of a healthy male subject.

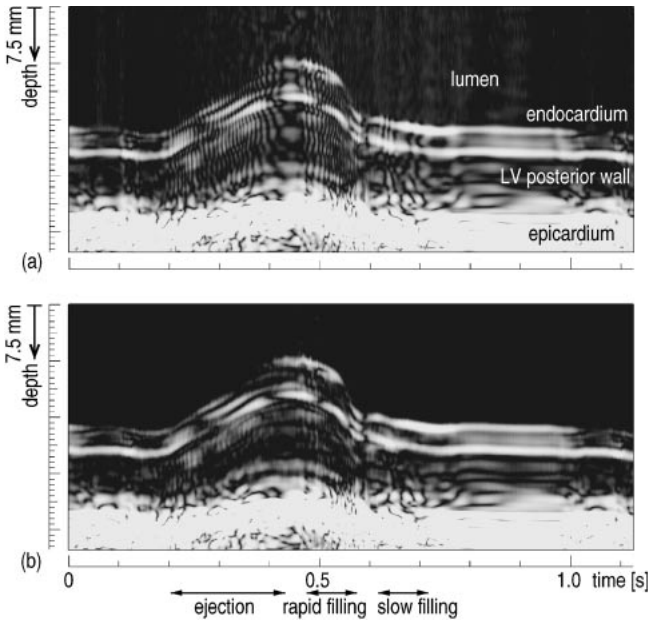

Fig. 10. M-mode images of the LV posterior wall. left: before correction, right: after correction.

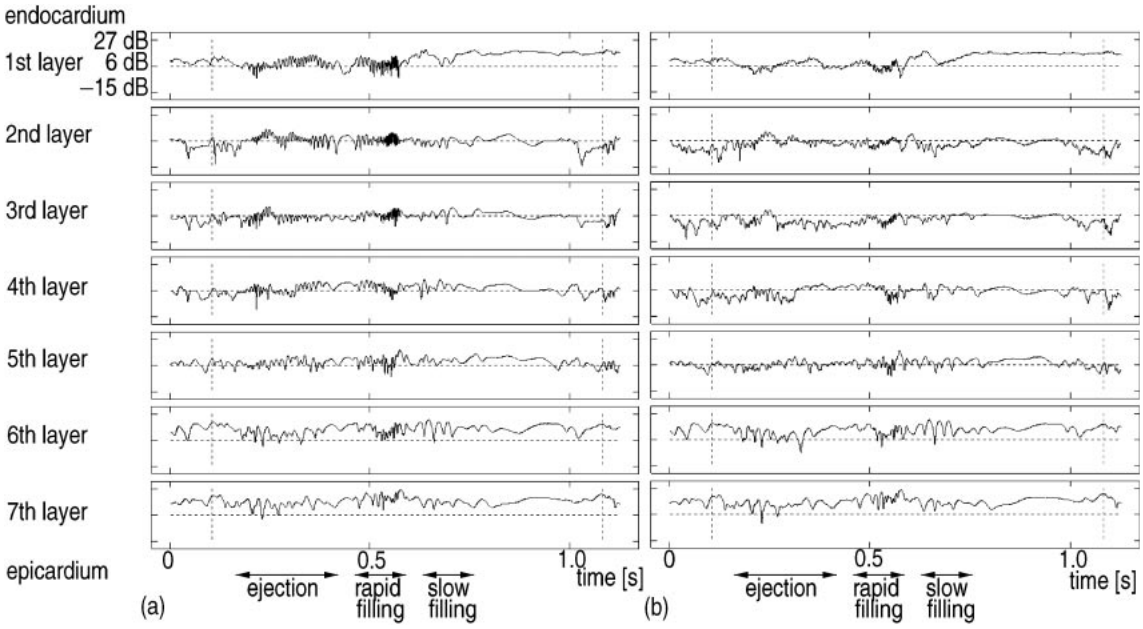

Fig. 11. IB signals for each of the 7 layers for the LV posterior wall. upper: before correction, lower: after correction.

in the rapid filling phase, and in the slow filling phase. By the correction, almost all these rapid components were eliminated in Figs. 10(b) and 11(b). In the region close to the endocardium, cyclic variation occurred, that is, the IB increased during diastole by about 10 dB from the IB values during systole.

5. Conclusions

In this paper, a method has been proposed to automatically track the position and the size of the ROI for calculating IB with high spatial and time resolution. By setting the ROI between two adjacent points, the position and the size of the ROI were automatically traced. Since spatial resolution and time resolution were increased to 1 mm and 200 μs, respectively, rapid variation components appeared in the IB signal for the first time. Such rapid components highly depend on the speed of change in thickness and these components are the result of interference among the waves reflected by scatterers other than the myocardium in the ROI. Thus, we have proposed a method for eliminating these rapid components by estimating the complex value of the bias components in the quadrature demodulated signal.

By applying the proposed method to a sponge phantom, the interference components were sufficiently suppressed. Next, the method was applied to the LV posterior wall of a healthy subject. The IB signal was measured with high time resolution and high spatial resolution, indicating that this method has potential for diagnosis of the vulnerability of the regional heart muscle.

1) B. Barzilai, E. I. Madaras, B. E. Sobel, J. G. Miller and J. E. Perez: Am. J. Physiol. **247** (1984) H478.
2) E. I. Madaras, B. Barzilai, J. E. Perez, B. E. Sobel and J. G. Miller: Ultrason. Imag. **5** (1983) 229.
3) R. M. Glueck, J. G. Mottley, J. G. Miller, B. E. Sobel and J. E. Perez: Circulation **68** (1983) III-330.
4) M. L. Marcus, R. E. Kerber, J. Ehrhardt and F. M. Abboud: Circulation **52** (1975) 254.
5) S. A. Wickline, L. J. Thomas III, J. G. Miller, B. E. Sobel and J. E. Perez: Circulation **72** (1985) 183.
6) S. A. Wickline, L. J. Thomas III, J. G. Miller, B. E. Sobel and J. E. Perez: Circulation **74** (1986) 389.
7) S. Nozaki, A. N. DeMaria, G. A. Helmer and H. K. Hammond: Circulation **92** (1995) 2676.
8) S. Takiuchi, H. Ito, K. Iwakura, Y. Taniyama, N. Nishikawa, T. Masuyama, M. Hori, Y. Higashino, K. Fujii and T. Minamino: Circulation **97** (1998) 356.
9) H. Kanai, M. Sato, Y. Koiwa and N. Chubachi: IEEE Trans. Ultrason. Ferroelectr. & Freq. Control **43** (1996) 791.
10) H. Kanai, H. Hasegawa, N. Chubachi, Y. Koiwa and M. Tanaka: IEEE Trans. Ultrason. Ferroelectr. & Freq. Control **44** (1997) 752.
11) J. G. Mottley, R. M. Glueck, J. E. Perez, B. E. Sobel and J. G. Miller: J. Acoust. Soc. Am. **76** (1984) 1617.
12) B. Hete and K. K. Shung: IEEE Trans. Ultrason. Ferroelectr. & Freq. Control **40** (1993) 354.
13) C.-Y. Wang and K. K. Shung: IEEE Trans. Ultrason. Ferroelectr. & Freq. Control **45** (1998) 504.